RSC Advances

ROYAL SOCIETY OF CHEMISTRY

www.rsc.org/advances

Cite this: DOI: 10.1039/c0xx00000x

www.rsc.org/xxxxxx

ARTICLE TYPE

Interfacial healing of carbon fiber composites in the presence of gold nanoparticles as localized "nano-heaters"

Zhenxing Cao[a], Rongguo Wang*[a], Lifeng Hao[a], Weicheng Jiao[a], Fan Yang[a], Qi Wang[a], Wenbo Liu[b], Boyu Zhang[a], Xiaolong Lu[a], Xiaodong He[a]

Received (in XXX, XXX) Xth XXXXXXXXX 20XX, Accepted Xth XXXXXXXXX 20XX
DOI: 10.1039/b000000x

In this paper, interfacial healing was achieved in carbon fiber composites via local heating generated by photothermal effect of gold nanoparticles (Au NPs). The interfacial damage can be locally repaired by melting polymethyl methacrylate and re-infiltrating carbon fiber to form a new interface. The Au NPs were coated on carbon fibers by electrophoretic depositions as nano-heaters and the coating density was controlled by varying the electrophoresis time. The healing ability was confirmed in the micro bond test by comparing the interfacial shear strength and surface morphology of the samples before and after healing. Experimental results showed that coating density of Au NPs and irradiation intensity played a key role. Repeated healings can be achieved with only a small reduction in interfacial strength.

INTRODUCTION

Interfaces play an important role in the mechanical properties of fiber-reinforced composites[1-3]. In continuous fiber-reinforced composites, the interfaces act as an intermediate bridge, which transfer load from the matrix to fibers through shear flow. Interfacial debonding is the dominant damage initiation mechanism, which tends to propagate along the interface after repeated loading, develops into large-scale damage and ultimately leads to failure of the whole composite. Traditionally, chemical and physical modifications of fiber surfaces have been used to improve interfacial adhesion and subsequent mechanical durability[4-6]. However, these methods are not adequate to prevent interfacial debonding to take place. To address this problem, a promising solution is to heal the damage to extend the lifetime of the composites. Many papers have reported self-healing materials[7-12], however most of them focused on repairing large scale delaminations and matrix cracking, with little attention paid to interfacial healing at early stage[13-15]. Here, we presented a novel method for local healing of the interface of carbon fiber reinforced thermoplastic composite in nanoscale using the photothermal effect of gold nanoparticles (Au NPs).

The photothermal effect of Au NPs refers to surface plasmon resonance mediated heating, whereby the incident light energy converts into heat[16]. The light absorbed by the nanoparticle generates a nonequilibrium electron distribution that decays by electron− electron scattering. The heated electron gas cools down rapidly by exchanging energy with the nanoparticle lattice[17], and the particle temperature rises significantly, heating the local environment. The photothermal effect in the Au NPs caused by the adsorption of light is emerging as a powerful tool in the manipulation of nanoscale thermally activated processes, which has been utilized for photothermal cancer therapy[18-22], drug delivery[23, 24], chemical deposition[25, 26], nanolithography[27, 28] and nanoscale patterning[29, 30]. Recent published work has utilized photothermal heating to achieve local heating through incorporation of these "nanoheaters" into the solid matrix, with the ability to thermally treat one subset of a sample and leave the remainder unchanged[31-37]. Thus this method is an excellent candidate for accurately local healing. Hongji Zhang et al. demonstrated a general method for preparing a light-healable strong hydrogel and fast optical healing of crystalline polymers[38, 39].

In this paper, we fabricated Au NPs coated carbon fibers and tested its healing ability in micro bond test. Au NPs were deposited onto the surface of carbon fibers by electrophoretic deposition (EPD) method, and the Au NPs coated carbon fibers were used to make micro bond test samples by placing polymethyl methacrylate (PMMA) droplet onto it. In order to confirm the healing ability, the resin droplet was pulled off first to induce interfacial debonding and followed by laser irradiate healing. This process was applied to a single droplet for several times for repeated healing. The healing mechanism was discussed and the influences of some key factors such as Au NPs density and laser irradiation were investigated.

EXPERIMENTAL SECTION

Fabrication of Au NPs

Citrate-stabilized Au NPs were synthesized by using the Frens method[40]. The chlorauric acid (0.01 wt%, J&K Chemical Ltd) was first mixed with 200 ml tripled distilled water in a 500 ml

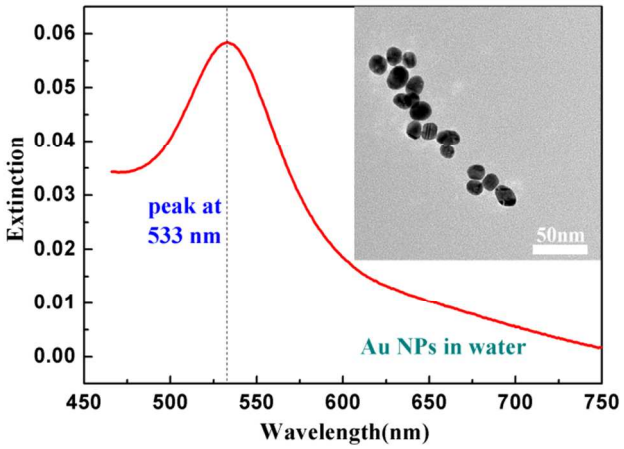

Fig. 1 Extinction measurements of Au NPs dispersed in water displaying a peak at 533 nm labeled by a vertical dashed line. Inset: TEM image of the Au NPs with diameter of 20 ± 5 nm.

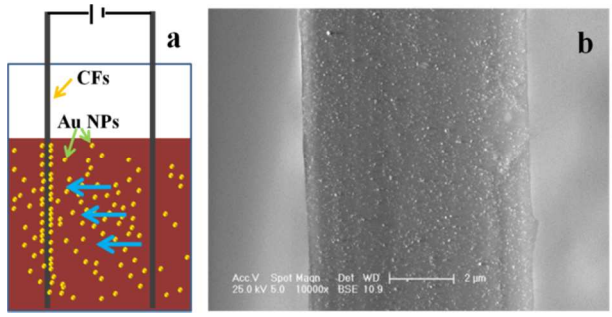

Fig. 2 (a) Schematic of the experimental setup of EPD. (b) SEM image of Au NPs coated carbon fiber with 25 min electrophoresis time.

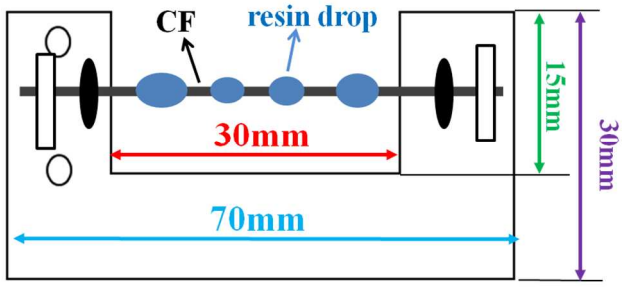

Chart 1. Scheme of micro bond test specimen.

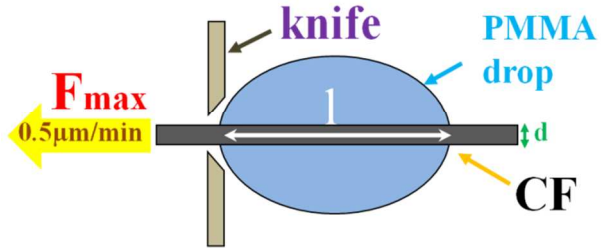

Chart 2. Sketch of micro bond test

round-bottom flask, and the solution was heated to boiling. Then the aqueous trisodium citrate (1.0 wt%, 10 ml, J&K Chemical Ltd) was quickly injected into the boiling solution, which turns its colour from blue to brilliant red after approximate 100 s, indicating the formation of Au NPs. Dry polyvinyl pyrrolidone (J&K Chemical Ltd) in an amount equal to that of the chlorauric acid was added to the solution to stabilize the nanoparticles further. The citrate-stabilized Au NPs were characterized by TEM (JEM-2100F, JEOL LTD) and showed a shape of sphere or slightly oblate sphere, with a diameter of 20±5 nm as shown in the inset of Fig. 1. The extinction spectrum of the Au NPs in water was measured to identify the location of the surface plasmon resonance with ultra-violet visible spectrometer (CARY 50 Scan), as shown in Fig. 1. The Au NPs dispersed in water have a single narrow plasmon resonance peak at 533 nm, and this result indirectly proved the good control of micromorphology of the Au NPs in the synthesis process.

Preparation of Au NPs coated carbon fibers

Au NPs were coated onto carbon fiber (T700-SC, Toray) surface by electrophoretic deposition method illustrated in Fig. 2 (a), in which carbon fiber bundles (anode) and graphite (cathode) were immersed in the Au NPs aqueous solution with a separation of 5cm. During deposition, a voltage of 8 v is applied between the two electrodes for 3 min, 5 min, 10 min and 25 min. The voltage tends to create an electric field between the two electrodes and drive Au NPs, which possess a net negative charge, moving toward the carbon fiber bundles and depositing onto them. After EPD, the coated fiber bundles were immediately withdrawn from the solution and dried at 120 ℃ for 10 min. Fig. 2 (b) showed the SEM image of the Au NPs coated carbon fibers, measured by SEM (Quanta200F , FEI). It is clear that high yield Au NPs are uniformly distributed on the sample surface without apparent aggregations.

Preparation of micro bond test specimens

The carbon fiber reinforced PMMA (J&K Chemical Ltd) composite (CF/PMMA) was prepared for micro bond test. First a single filament was picked out of the Au NPs coated fiber bundles, and fastened to a U shaped thin paper holder (30×70 mm) with double sided adhesive tape as shown in Chart 1, leaving a free fiber length of approximately 30 mm. Then PMMA/chloroform at a weight ratio of 1:20 was placed onto the fiber filament with a sharp needle, forming many microdroplets with an embedded length ranging from 40–120 μm. Finally, the specimen was shaped in an air dry oven under normal pressure at 200 ℃ for 30 min.

Interfacial de-bonding and healing procedure

Interface de-bonding was induced by the micro bond test with interface strength tester (MODEL HM410, TOHEI SANGYO) as schematic shown in Chart 2, in which two knives are brought together to form a gap smaller than the diameter of the resin droplet. In the experiment, the carbon fiber is pulled horizontally with the resin droplet against the gap. The knives deform the droplet inducing a shear force along the fiber droplet interface and eventually pull off the droplet causing an interfacial debonding. Meanwhile, a load displacement curve from each test was recorded and interfacial shear strength (IFSS), τ, can be calculated as:

$$\tau = \frac{F_{\max}}{\pi d l} \quad (1)$$

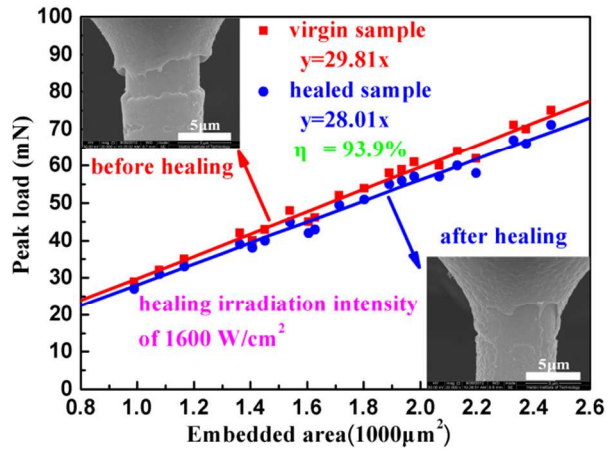

Fig. 3 Plots of peak force versus embedded area measured for sample with 25 min electrophoresis time before and after healing using micro bond test. The healing efficiency was 93.9% calculated by IFSS obtained from the slope of the fitted straight lines. The SEM images compare the surface micromorphology of deformed sample before healing (upper left inset) and healed sample after healing (lower right inset) with irradiation intensity of 1600 W/cm^2.

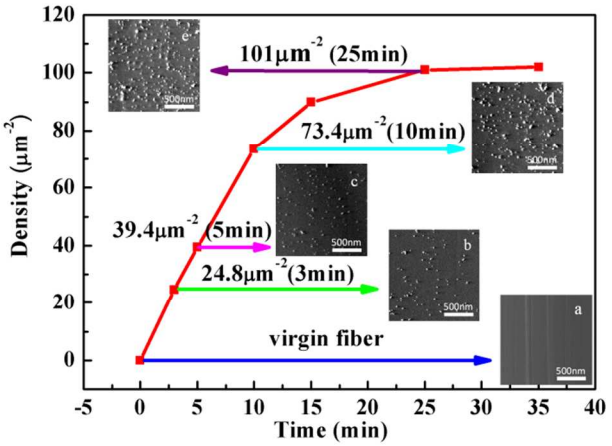

Fig. 4 Evolution of Au NPs density versus electrophoresis time. The density increased linearly with the time before 10 min and reached saturation at 25 min with Au NPs density of 101μm^{-2}. The SEM image (a) is virgin fiber surface for comparison and (b-e) are Au NPs coated fibers surface with different electrophoresis times.

where Fmax is the maximum force, d is the corresponding fiber diameter and l is embedded length.

The debonded sample was irradiated by a 532 nm continuous-wave diode laser with the power of 150 mw for 10 min. The laser energy is converted into heat via photothermal effect and healing the interface damage. The irradiation intensity can be varied from 100 to 2000 W/cm^2 by changing the beam size. The aforementioned melt processes were repeated for several times for a single droplet to test the repeated healing capability. The healing efficiency is defined as the interfacial shear strength ratio between the healed and the virgin sample.

$$\eta = \frac{\tau_{\text{Healed}}}{\tau_{\text{Virgin}}} \qquad (2)$$

To determine the healing efficiency accurately, de-bonding and healing were repeatedly applied to more than twenty samples.

RESULTS AND DISCUSSION

Photothermal effect for interfacial healing

The left and right insets of Fig. 3 show the SEM images of a resin droplet before and after healing. There is apparent debonding between the carbon fiber and PMMA resin before healing. We can see the carbon fiber exposure at the debonding position. After irradiating healing 10 min with a laser of 1600 W/cm^2, the morphology of the deformed sample is significantly modified at the debonding position and it is clear that the exposed fiber was recovered by PMMA. There is a new interface formed by the mechanical interlock between the fiber and PMMA. The IFSS of the newly created interface was also measured. Fig. 3 shows the plot of peak force as a function of embedded area of droplets. The IFSS, obtained from the slopes of the fitted straight lines in according to equation (1), are 29.81 MPa and 28.01 MPa for the virgin sample and healed one, revealing healing efficiency of η = 93.9%.

It is clearly that not only the morphology but also the mechanical property of the interface is recovered. In order to rule out other factors such as direct laser heating of the resin, the same experiment was performed with a microdroplet sample using a virgin carbon fiber without the Au NPs coating. Although the virgin IFSS is almost the same as fibers coated with Au NPs, we did not observe apparent recovery of IFSS, which indicated that the laser intensity is not sufficient to melt the resin and the interface healing process solely relies on the rising of the temperature generated by the local photothermal effect of the Au NPs.

It is also noted, from the IFSS measurement of the virgin and healed sample, that healing efficiency of 93.9% can be achieved, exceeding many other self-healing methods. We believe that this is due to the special local heating distribution of Au NPs. After absorption of the photon energy by the Au NPs placed around the interface, a large amount of heat was accumulated by the Au NPs, which can raise the local temperature to above the melting temperature T_m of the PMMA. As a result, the crystallites are melted and PMMA chains in the melt can diffuse across the interface. Once turning off the light, diffused PMMA chains can recrystallize during the cooling, which leads the fiber and PMMA bonded together forming mechanical interlock as shown in Fig. 3. At the same time, the thermal expansion at the interface due to the local heating was blocked by the surrounding cold matrix which makes PMMA "hug" fiber tightly, producing radial press. The mechanical interlock and radial press will contribute interfacial friction to recover the IFSS[41]. As a result, the interface damage is healed and IFSS is recovered.

Effect of coating density of Au NPs on the healing efficiency

The coating density of Au NPs is an important factor in the healing process induced by photothermal effect and could be varied by changing the electrophoresis time while keeping other parameters constant. The insets of Fig. 4 show the SEM images of the virgin and the Au NPs coated fibers after electrophoresis deposition for 3 min, 5 min, 10 min and 25 min. The coating density was measured by counting the number of Au NPs in each image and plotted as a function of the electrophoresis time, as shown in Fig. 4. It could be noted that the density of Au NPs increased linearly to a value of 73.4 μm^{-2} for the first 10 min, in

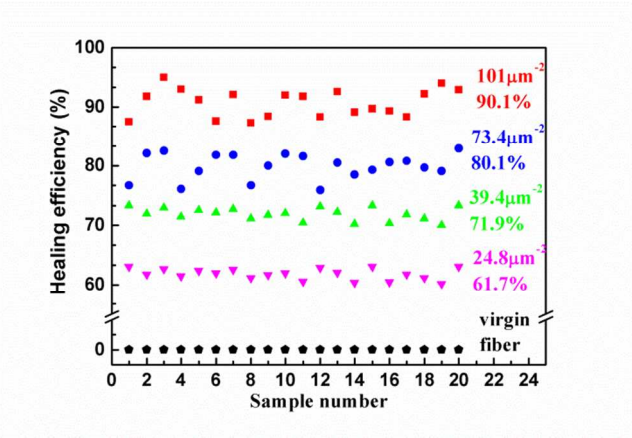

Fig. 5 The healing efficiency for samples with different coating density under healing irradiation intensity of 1400 W/cm^2.

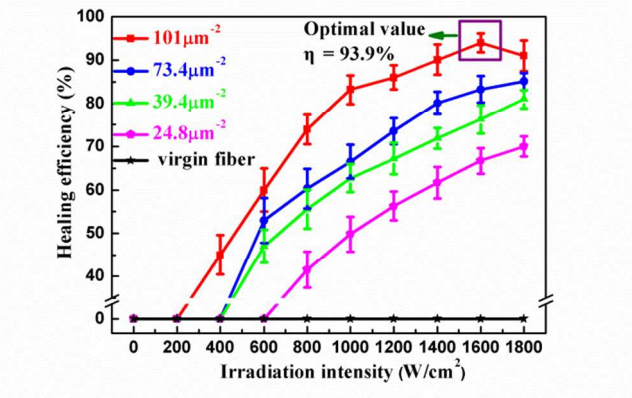

Fig. 6 Healing efficiency attained as a function of irradiation intensity for samples with different coating density. For comparison, the result of blank sample with no Au NPs present is also presented.

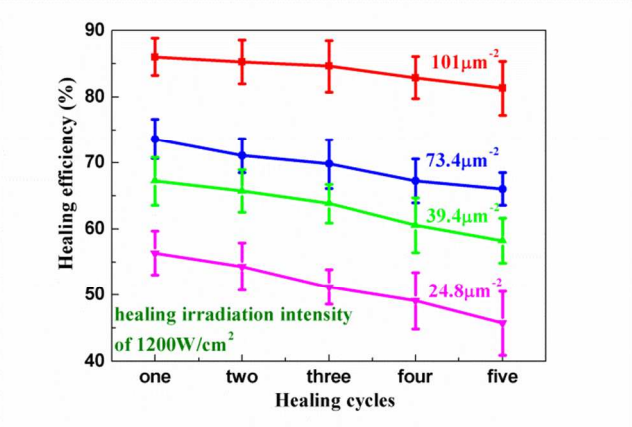

Fig. 7 The healing efficiency versus healing cycles by irradiation intensity of 1200 W/cm^2.

accordance with the Hamakers law which could be expressed as

$$w = \int_{t_1}^{t_2} \mu \cdot E \cdot A \cdot C \cdot dt \quad (3)$$

where w is the deposit yield which is proportional to the density, μ is the electrophoretic mobility, E is the electric field strength, A is the surface area of the electrode, C is the particle mass concentration in the suspension and t is the electrophoresis time. From equation (3), it is clear that the coating density is proportional to the electrophoresis time. After 10 min, the deposition rate decreased and the coating density eventually saturated at 101 μm^{-2} for an electrophoresis time of 25 min. This might be ascribed to the balance between the repulsive electrostatic forces and the attractive Van der Waals force.

Twenty samples are prepared for each electrophoresis time, and used in the aforementioned healing experiments. Fig. 5 shows efficiency of the sample under a laser irradiation of 1400 W/cm^2. It is found that the value of the healing efficiency are quite close for the samples prepared with the same electrophoresis time, indicating that both the electrophoresis deposition process and the heating process are stable and repeatable. For the blank sample, the healing efficiency is about 0, further conforming that the interfacial damage healing capability comes from the photothermal effect of the Au NPs. For Au NPs coated samples, the healing efficiency increases monotonously from 61.7% for the samples with the coating density of 24.8 μm^{-2} to 90.1% for the saturated samples with the density of 101 μm^{-2}. This result is reasonable, since with the increase of the coating density, the number of the Au NPs at the interface increases as well, which tends to convert more photo energy into heat and melt more resin, resulting in a better infiltration to the carbon fiber. At the same time, the extra heat is likely to raise the temperature at the interface, causing the molecular chain of the resin to move more intensively and eventually improving the healing process. From the result mentioned above, it is clear that the samples with the largest coating density provide the best heating efficiency and recover most of the IFSS.

Effect of irradiation intensity on the healing efficiency

Fig. 6 shows healing efficiency as a function of the irradiation intensity for carbon fibers with different coating densities，which is zero for the blank sample and shows the same trend for all other Au NPs coated ones. The healing process is initialized when the irradiation intensity reached a certain threshold and the healing efficiency increases monotonically with further increase of the irradiation intensity. It is also found that the higher coating density the smaller threshold is. This behavior might be explained by the temperature variations at the interface, which are proportional to both the irradiation intensity and the coating density theoretically[42, 43]. Hence, by using stronger irradiation, the temperature at the interface rises as well. However, the healing process could not be triggered until the temperature exceeded the melting temperature of the resin at which point the resin start to acquire mobility. This causes a threshold that decreases with the increase of the coating density of Au NPs. By increasing the irradiation intensity further, more resin was melted, boosting the healing efficiency. It is also noted that there exists a droop of the healing efficiency for the saturated sample (101μm^{-2}) under the irradiation above 1600 W/cm^2. This might be attributed to the thermal decomposition of the resin which tends to produce new interfacial damage. From the discussion above, we figure out that the optimized healing condition is achieved for the saturated samples under irradiation intensity of 1600 W/cm^2.

Repeated healing of interface

Repeated healing is highly desired since it can dramatically

extend the lifetime of composite materials. In the experiment, we test the capability of repeated healing by the photothermal effect of Au NPs under an irradiation intensity of 1200 W/cm^2. Fig. 7 shows the average healing efficiency as a function of the healing cycles for samples with different coating densities. We note, surprisingly, that even after five cycles the IFSS could be recovered to 45.7%, 58.2%, 66.1% and 81.3% of its original value for the samples with the density of 24.8 μm^{-2}, 39.4 μm^{-2}, 73.4 μm^{-2} and 101μm^{-2} respectively. It is also noted that there is a small degradation for all the samples which might be ascribed to the lost of the Au NPs during the pulling off process before each healing cycle.

Conclusions

In conclusion, we have demonstrated a facile method for interfacial healing of carbon fiber composites based on photothermal effect of the Au NPs and investigated its influence factors such as coating densities of Au NPs and irradiation intensity. Healing efficiency as high as 93.9% is achieved under optimized conditions. This method has several advantages. First, Au NPs, selectively placed in the interface region is capable to locally heal the interfacial debonding without significantly affecting the remainder of the material. This makes it possible to repair a certain region in composites via modifying the irradiation position and spot size. Second, heat is homogenous generated inside the derived healing regions avoiding the temperature gradient induced by conventional heating method which always has the surface get warm first. Third, the healing process can be carried out repeated, which can dramatically extend the lifetime of healed composites. Although the healing experiments are performed in carbon fiber reinforced PMMA system, the method can be easily applied to other fiber reinforced thermoplastic composites with a broader resin selection over the conventional photo induced healing and have a great potential in a wide variety of application ranging from microelectronics to aerospace.

ACKNOWLEDGMENT

The works were financially supported by the fund of the National Basic Research Program of China (No.2011CB605605), Science and Technology on Advanced Composites in Special Environments Laboratory of China (No.9140C490107130C49184) and Ph.D. Programs Foundation of Ministry of Education of China (No.20122302120033).

Notes and references

[a] *Center for Composite Materials and Structures, Harbin Institute of Technology, Harbin, 150080, China. Fax: +86-0451-86402399; Tel: +86-0451-86402399; E-mail: wrg@hit.edu.cn*
[b] *School of Materials Science and Engineering, Harbin Institute of Technology, Harbin, 150001, China. Fax: +86-0451-86402625; Tel: +86-0451-86402625; E-mail: liuwenbo@hit.edu.cn*

1. B. Pukanszky, *Eur Polym J*, 2005, **41**, 645-662.
2. F. R. Jones, *J Adhes Sci Technol*, 2010, **24**, 171-202.
3. M. Zhou, J. J. Yan, Y. H. Li, C. Z. Geng, C. He, K. Wang and Q. Fu, *Rsc Adv*, 2013, **3**, 26418-26426.
4. X. D. He, F. H. Zhang, R. G. Wang and W. B. Liu, *Carbon*, 2007, **45**, 2559-2563.
5. S. Zhang, W. B. Liu, L. F. Hao, W. C. Jiao, F. Yang and R. G. Wang, *Compos Sci Technol*, 2013, **88**, 120-125.
6. X. Q. Zhang, H. B. Xu and X. Y. Fan, *Rsc Adv*, 2014, **4**, 12198-12205.
7. R. G. Wang, H. Y. Li, H. L. Hu, X. D. He and W. B. Liu, *J Appl Polym Sci*, 2009, **113**, 1501-1506.
8. D. Y. Wu, S. Meure and D. Solomon, *Prog Polym Sci*, 2008, **33**, 479-522.
9. G. Lykotrafitis, A. J. Rosakis and G. Ravichandran, *Science*, 2006, **313**, 1765-1768.
10. Y. C. Yuan, X. J. Ye, M. Z. Rong, M. Q. Zhang, G. C. Yang and J. Q. Zhao, *Acs Appl Mater Inter*, 2011, **3**, 4487-4495.
11. R. P. Wool, *Soft Matter*, 2008, **4**, 400-418.
12. E. Koh, N. K. Kim, J. Shin and Y. W. Kim, *Rsc Adv*, 2014, **4**, 16214-16223.
13. K. Sanada, I. Yasuda and Y. Shindo, *Plast Rubber Compos*, 2006, **35**, 67-72.
14. B. J. Blaiszik, M. Baginska, S. R. White and N. R. Sottos, *Adv Funct Mater*, 2010, **20**, 3547-3554.
15. A. R. Jones, A. Cintora, S. R. White and N. R. Sottos, *Acs Appl Mater Inter*, 2014, **6**, 6033-6039.
16. S. Link and M. A. El-Sayed, *Int Rev Phys Chem*, 2000, **19**, 409-453.
17. S. A. Maier and H. A. Atwater, *J Appl Phys*, 2005, **98**.
18. P. K. Jain, I. H. El-Sayed and M. A. El-Sayed, *Nano Today*, 2007, **2**, 18-29.
19. H. C. Huang, K. Rege and J. J. Heys, *Acs Nano*, 2010, **4**, 2892-2900.
20. Y. L. Luo, Y. S. Shiao and Y. F. Huang, *Acs Nano*, 2011, **5**, 7796-7804.
21. S. T. Wang, K. J. Chen, T. H. Wu, H. Wang, W. Y. Lin, M. Ohashi, P. Y. Chiou and H. R. Tseng, *Angew Chem Int Edit*, 2010, **49**, 3777-3781.
22. X. C. Wang, G. H. Li, Y. Ding and S. Q. Sun, *Rsc Adv*, 2014, **4**, 30375-30383.
23. H. Y. Liu, T. L. Liu, X. L. Wu, L. L. Li, L. F. Tan, D. Chen and F. Q. Tang, *Adv Mater*, 2012, **24**, 755-+.
24. D. Pissuwan, T. Niidome and M. B. Cortie, *J Control Release*, 2011, **149**, 65-71.
25. D. A. Boyd, L. Greengard, M. Brongersma, M. Y. El-Naggar and D. G. Goodwin, *Nano Lett*, 2006, **6**, 2592-2597.
26. W. H. Hung, I. K. Hsu, A. Bushmaker, R. Kumar, J. Theiss and S. B. Cronin, *Nano Lett*, 2008, **8**, 3278-3282.
27. N. Stokes, A. M. McDonagh and M. B. Cortie, *Gold Bull*, 2007, **40**, 310-320.
28. M. B. Cortie, N. Harris and M. Ford, *Physica B*, 2007, **394**, 188-192.
29. A. U. Zillohu, R. Abdelaziz, M. K. Hedayati, T. Emmler, S. Homaeigohar and M. Elbahri, *J Phys Chem C*, 2012, **116**, 19611-19611.
30. C. D. Jones and L. A. Lyon, *J Am Chem Soc*, 2003, **125**, 460-465.
31. H. J. Zhang, H. S. Xia and Y. Zhao, *J Mater Chem*, 2012, **22**, 845-849.
32. S. Maity, L. N. Downen, J. R. Bochinski and L. I. Clarke, *Polymer*, 2011, **52**, 1674-1685.
33. S. Maity, J. R. Bochinski and L. I. Clarke, *Adv Funct Mater*, 2012, **22**, 5259-5270.

34. H. J. Zhang and Y. Zhao, *Acs Appl Mater Inter*, 2013, **5**, 13069-13075.
35. V. Viswanath, S. Maity, J. R. Bochinski, L. I. Clarke and R. E. Gorga, *Macromolecules*, 2013, **46**, 8596-8607.
36. Y. B. Li, T. Verbiest, R. Strobbe and I. F. J. Vankelecom, *J Mater Chem A*, 2014, **2**, 3182-3189.
37. S. Maity, K. A. Kozek, W. C. Wu, J. B. Tracy, J. R. Bochinski and L. I. Clarke, *Part Part Syst Char*, 2013, **30**, 193-202.
38. H. J. Zhang, D. H. Han, Q. Yan, D. Fortin, H. S. Xia and Y. Zhao, *J Mater Chem A*, 2014, **2**, 13373-13379.
39. H. J. Zhang, D. Fortin, H. S. Xia and Y. Zhao, *Macromol Rapid Comm*, 2013, **34**, 1742-1746.
40. G. Frens, K. Z., J. Turkevich, J. Hillier and P. C. Stevenson, *nature physical science*, 1973, **241**, 20-22
41. J. L. Thomason and L. Yang, *Compos Sci Technol*, 2011, **71**, 1600-1605.
42. A. O. Govorov, W. Zhang, T. Skeini, H. Richardson, J. Lee and N. A. Kotov, *Nanoscale Res Lett*, 2006, **1**, 84-90.
43. A. O. Govorov and H. H. Richardson, *Nano Today*, 2007, **2**, 30-38.